DUAL POROSITY MODELS OF A DISCHARGE TEST

Jaime Jemuel C. Austria, Jr.[1, 2] and Michael J. O'Sullivan[2], and John Doherty[3]

[1]Energy Development Corporation, 38/F One Corporate Centre Building,

Julia Vargas corner Meralco Avenue, Pasig 1605 Philippines

[2]Department of Engineering Science, The University of Auckland, Auckland 1010 New Zealand

[3]Watermark Numerical Computing, Brisbane, Australia

austria.jjc@energy.com.ph; m.osullivan@auckland.ac.nz; johndoherty@ozemail.com.au

Keywords: *Geothermal, numerical simulation, dual porosity models, MINC, discharge test, Fushime.*

ABSTRACT

The research reported here is part of a general study aimed at determining when dual-porosity models should be preferred ahead of single porosity models for modelling geothermal systems. A discharge test of well, SKG9D, in Fushime, Japan, was simulated using both single and dual porosity (MINC) models and inverse modelling was used to estimate parameters such as permeability, porosity and initial pressure and gas saturation.

The forward simulations were carried out with AUTOUGH2 (Yeh *et al.*, 2012), a modified version of TOUGH2 (Pruess *et al.*, 1999) while the inverse problem of determining the best-fit parameters for the models was solved using PEST (Doherty, 2013). The data used for calibration were flowing enthalpies and pressures measured daily for 139 days.

The results were compared for a single porosity model and various dual porosity (MINC) models with the aim of determining whether or not one type of model clearly fitted the data better than the others. All the dual porosity models used to simulate the discharge test of well SKG9D were able to reduce the objective function to a lower value than that for the single porosity model.

1. INTRODUCTION

The main objective of this work is to determine how a single porosity and a dual porosity model compare for modelling a discharge test. The discharge test data for this study was taken from well SKG9D in the Fushime geothermal field which is located in a depression along the coast line in the south eastern extremity of the Satsuma Peninsula or Satsunan area in Kyushu, Japan (as shown in Figure 1). The Fushime geothermal field is characterised by very high reservoir temperatures (>350°C) and high salinity of the production fluid (Okada and Yamada, 2002). The main geothermal reservoir of the Fushime geothermal system was formed along fractured zones inside and surrounding a dacite intrusion (Okada and Yamada, 2002; Okada *et al.*, 2000).

The fracture systems in the Fushime geothermal system are considered to be influenced by the intrusion and the major faults around the depression. The dacite intrusion is found at the centre of the depression which is outlined by major faults. The wells derive their permeability from these intrusions and major faults. The delineation of the distribution and knowledge of the characteristics of the fractures related to the intrusion are important in determining the behaviour of the geothermal system (Okada and Yamada, 2002; Okada *et al.*, 2000).

The discharge test data showed that SKG9D is a high-enthalpy and steam-dominated well. According to Pritchett (2005), such a high-enthalpy and steam-dominated discharge are related to local heterogeneity in the reservoir with a sharp permeability contrast between a relatively impermeable rock matrix and fracture zones, and he further concluded that dual porosity models are required for simulating this type of behaviour. This provided the motivation for using both dual and single porosity models for simulating the discharge behaviour of well SKG9D.

Figure 1: Location of Fushime geothermal field, modified after Okada and Yamada (2002)

In the single porosity approach, the fractured rock is represented as an equivalent, single continuum, possibly non-uniform and anisotropic. In contrast, the dual porosity model (Barenblatt *et al.*, 1960; Warren and Root, 1963) mathematically idealizes the flow region as two interacting media, namely, the fractures and the matrix. The MINC or multiple interacting continua method (Pruess and Narasimhan, 1982) which is a generalisation of the dual porosity approach is used in the present study. With the MINC method the matrix can be subdivided by using a nested sequence of blocks (Narasimhan, 1982).

Models having different fracture volume fractions and different numbers of blocks representing the matrix were tested. Previous work has shown that enthalpy transients for a production well show sensitivity to the choice of fracture volume fraction and matrix permeability (Austria and O'Sullivan, 2012).

2. MODELLING APPROACH

2.1 Model description

A simple single-layer radially symmetric grid was created. The radial model has a thickness of 200 m. The outer radius of the grid was chosen to be large enough (70.11 km) so that the model is infinite acting, with no changes in the outer blocks observed in any of the simulations. For the dual porosity model, the secondary mesh for the embedded matrix blocks which are required to accurately represent flow between the fracture and the rock matrix was created with GMINC (Pruess, 2010). The partitioning of the matrix was made in such a way that the first volume fraction corresponds to the fracture while the remainder of the volume was assigned to the matrix. The grid for the single porosity medium was used as the basis for the MINC model, as shown in Figure 1.

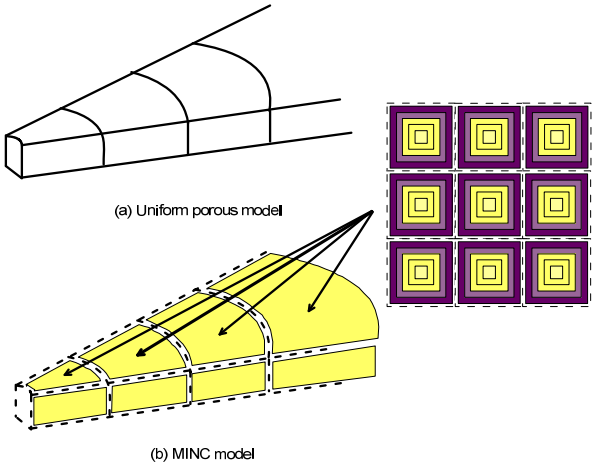

Figure 1: Block layout for the radial models

Nine MINC models were investigated, with three forms of grid partitioning, namely: *(1)* with a fracture volume fraction of $1x10^{-3}$ while the rest of the volume was divided into 4 matrix blocks; *(2)* with a fracture volume fraction of $1x10^{-3}$ while the rest of the volume was assigned to a single matrix block; and *(3)* with a fracture volume fraction of $1x10^{-2}$ while the rest of the volume fraction was assigned to a single matrix block. The MINC models were also created to represent the fracture volume in three different ways, namely: *(a)* as a single fracture with a very high porosity fixed at 99%; *(b)* as a fracture zone containing some rock material with a porosity fixed at 10%; and *(c)* as a fracture zone containing some rock material with variable fracture porosity. In *(c)*, the fracture porosity was selected as one of the parameters to be estimated by PEST. A detailed description of these MINC models is presented in Section 4.

The initial matrix porosity was chosen such that effective porosity of the MINC model was the same as the porosity of the single porosity model (see equation below):

$$por_{eff} = por_{frac} V_f + por_{mtrx}(1 - V_f)$$

A matrix porosity value of 4% was assigned for the single porosity model. For the fracture types in *(a)* and *(b)*, the dual porosity models were given an initial matrix porosity of 3.97% and 3.93% respectively when the fracture volume fraction was $1x10^{-3}$ and 3.94% and 3.04% respectively when the fracture volume fraction was $1x10^{-2}$. As a first estimate the single porosity model was given a permeability of 5 millidarcy (mD). The initial estimate of fracture permeability was retained at 5mD and the matrix permeability was assigned a value of 1mD for the dual porosity model.

The parameters that were given to PEST to be estimated varied for the different models but generally included the matrix and fracture permeability, matrix and fracture porosity, and initial pressure and gas saturation. During parameter estimation, the values of these parameters were adjusted by PEST to improve the match of the model results to the data.

The linear permeability function with residual immobile liquid and gas saturation values of 0.5 and 0.0 was assigned. The first-estimate initial conditions used were a pressure of 105 bars and a gas saturation of 0.25. The forward simulations were carried out with a time step sequence, which began with a very small time step then increased by a factor of two at every step until it reached a maximum of 0.5 day (Δt_1 = 21.1 s, $\Delta t_2 = 2\Delta t_1$, $\Delta t_3 = 2\Delta t_1$, ... $\Delta t_{n+1} = 2\Delta t_2$). The model was run to an end time of 139 days. The parameters used in the model are summarized in Table 1.

Table 1: Initial dual porosity model parameters

Parameters	Fracture	Matrix
Permeability	5 mD	1 mD
Porosity	99%	(i) 3.97%, 3.93% (ii) 3.94%, 3.04%
Rock grain density	$2500kg/m^3$	
Rock specific heat	1000J/kg K	
Rock conductivity	2.5W/m K	
Relative permeability	Linear: S_{lr}=0.50, S_{vr}=0	
Wellbore radius	0.1 m	
Initial conditions	Pressure =105 bars, gas saturation =0.25	

Note/s: Darcy is the unit for permeability, where 1 Darcy = $1 x10^{-12}$ m^2; *(i)* when $V_f = 1x10^{-3}$; *(ii)* when $V_f = 1x10^{-2}$.

2.2 Model parameters and calibration data

The AUTOUGH2 simulator (Yeh *et al.*, 2012), the University of Auckland's version of TOUGH2 (Pruess *et al.*, 1999) was used for solving the nonlinear mass and heat conservation equations. The permeability, porosity, and initial pressure and gas saturation were used as the model parameters to be adjusted to match the measured flowing enthalpy and pressure data. In addition, for the dual porosity models, the matrix and fracture permeability, matrix porosity, and in some cases fracture porosity were included as parameters to be estimated.

The model was calibrated against measurements of pressure and flowing enthalpy obtained during a 139 day discharge test. The well was shut three times during the 139 day period, at around days 48 to 50, day 55, and days 97 to 104. The early production rate averages around 3.3 kg/s but increased to 9.7 kg/s after day 105. The plot of production rate against time is shown in Figure 2.

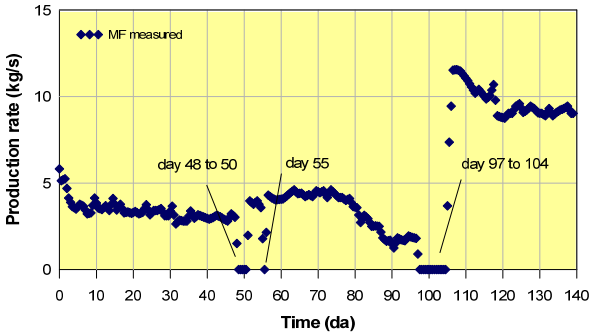

Figure 2: Production rate against time

2.3 Parameter estimation

The computer program PEST was used for estimating the parameters for the model that best fits the observed pressure and flowing enthalpy data. Before parameter estimation was performed, several forward runs of AUTOUGH2 were performed to ensure that the single and dual porosity models reached an end time of 139 days.

The PEST parameter estimation code was implemented as a wrapper around AUTOUGH2. PEST sets up successive input data files for AUTOUGH2, extracts results from the listing/output file using a PyTOUGH script (Croucher, 2011) to compare with the measured data, and systematically adjusts input parameter values. The extracted model results are then returned to be read by PEST, based on the instructions contained in the PEST instruction file. A PyTOUGH script was also used for deleting the listing files when the forward runs did not finish.

Whereas in manual calibration model parameters are estimated by trial-and error, PEST estimates the optimal parameter values by minimising the objective function calculated as the sum of weighted, squared, differences between simulated model values and data from field measurements. The objective function is minimised using truncated singular value decomposition supplemented, where necessary, with Tikhonov regularisation. It was decided to include all the parameters: permeability, porosity, initial pressure and initial gas saturation, and let PEST estimate their values.

After completing the required number of AUTOUGH2 forward runs, PEST calculates the derivative of each component of the objective function with respect to each parameter value by using finite differences. The matrix containing these derivatives is called the Jacobian. Thus, the model has to be run once to begin with and then once more for every parameter to be estimated. An increment, provided by the user, is added to the relevant parameter value prior to each additional run. The resulting change in the objective function is divided by this increment to calculate its derivative with respect to the parameter.

After each PEST optimisation run, the optimization algorithm, based on the truncated singular value decomposition method, adjusts the values of the model parameters to decrease the value of the objective function (Doherty, 2013; Finsterle, 2003). A more detailed discussion of the inversion methodologies implemented by PEST can be found in PEST documentation (Doherty, 2013).

The most common cause of a failure of PEST to find the minimum of the objective function is the effect of round-off errors in the calculation of derivatives (Doherty, 2013) hence a version of AUTOUGH2 which has an input file with an extra two decimal digits of precision for the permeability parameters was used. The extra precision input allowed PEST to pass higher precision parameters into AUTOUGH2 and ensured that the calculation of derivatives does not suffer because of the effect of round-off errors.

Parameter estimation was also carried out with AuiTough2, the University of Auckland's version of iTough2 (Finsterle, 2003). After several forward runs that did not finish were encountered, the experiments with AuiTough2 were discontinued and a switch was made to PEST because it has a scheme for handling model failures which allows parameter optimisation to continue even when the real system is highly stressed. There are variables in the PEST control file that can be set to accommodate a total or partial model failure during Jacobian evaluation runs and in testing the efficacy of trial parameter upgrades. The handling of model failures using PEST will be discussed in more detail in Section 3.1.

3. CHALLENGES WITH INVERSE MODELLING

Modelling the Fushime well SKG9D discharge test is a difficult problem for several reasons:

i. The forward model will not run until the target end time in some cases.

ii. The parameter estimation process is computationally demanding. In the beginning, when parameters were far from their optimum values, it took a forward run of AUTOUGH2 several hours to finish because some of the dual porosity models required very small time steps.

iii. There is the possibility that the minimization of the objective function may not give a global optimum but instead it may give a local optimum that may not be a "good solution" in the sense that the optimal parameters may not be what are expected, or what are found to be acceptable by the modeller.

PEST has features to address some of these difficulties. In the following section, the customisation of the PEST inversion process carried out to address these difficulties is discussed.

3.1 Scheme for rejecting model failures

It was found that the desirable region of parameter space is adjacent to a region of parameter space where the forward model will not run for the full 139 days. This is because at the end of the time period, when the flow rate is high, the real system is highly stressed giving a large pressure decline and a high enthalpy. A small decrease in permeability and porosity changes a numerically stable model to one for which the pressure drops unrealistically low and the simulation stops.

An example of this problem occurred with an initial trial using a 5-MINC block model with a fracture volume fraction of $1x10^{-3}$ and fixed fracture porosity of 99%. It was found that the simulation could not finish with a low fracture permeability (k_f < 1.2 mD) and a low matrix porosity (θ_{matrix} < 1.6%). Soon after day 105 the pressure in the production block AA 1 became extremely low (656 Pa) because there was not enough fluid moving into the production block due

to the very low permeability in the fracture and low porosity in the matrix. The results of a run that did not finish are shown in Figures 3 and 4. It is seen from Figures 3 and 4 that the AUTOUGH2 run ended prematurely after 105 days.

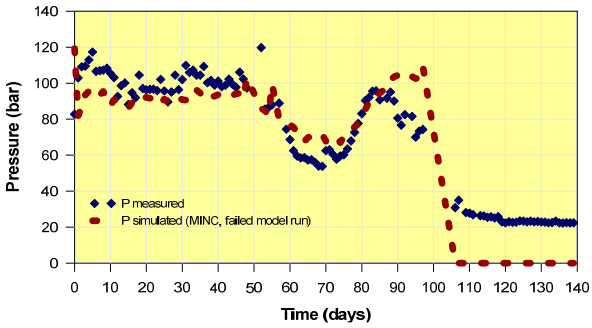

Figure 3: Feedzone pressure result for a failed dual porosity model simulation

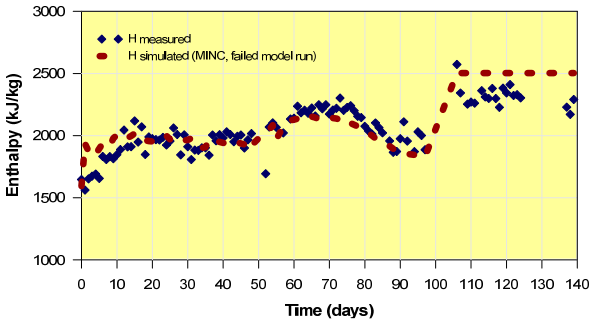

Figure 4: Flowing enthalpy result for a failed dual porosity model simulation

In order to reject AUTOUGH2 runs that do not reach the set end time, the "derforgive" and "lamforgive" variables were included in the PEST control file. The "derforgive" variable accommodates a total or partial model failure during a Jacobian calculation run by setting important parameter sensitivities to zero. With "derforgive", a "dummy" model output value is provided which does least harm to the derivative. On the other hand, the "lamforgive" variable treats a model run failure during testing of parameter upgrades in the lambda search as a high objective function. This provides PEST with a disincentive to use parameter values which are close in parameter space to those which have been demonstrated to result in problematical model behaviour.

These control file settings prevented the PEST simulation from approaching critically low permeability and porosity values that would cause the forward AuTOUGH2 runs to prematurely end. By rejecting unfinished model runs, these PEST settings ensured that the optimisation runs were terminated because the objective function could no longer be improved and not because of a series of failed forward runs.

3.2 Parallelisation

At the start of the simulation when parameters were far from their optimum values, it took a forward run of AUTOUGH2 several hours to finish because some of the dual porosity models require very small time steps. Besides this problem, a large computational time was required because four model runs are required per parameter as the 5-point derivative stencil was adopted to improve the accuracy of the calculation of derivatives.

To speed up the parameter estimation process, parallelisation of the AUTOUGH2 model runs was adopted by implementing a special version of parallel PEST called BeoPEST (Schreüder, 2009). BeoPEST creates an improvised cluster on the fly. The cluster can be any set of computers able to communicate via an internet connection.

In BeoPEST, the master process performs the parameter estimation, sends the parameters to be used by the model to the subordinate cluster, and receives model results back from the subordinate in binary form via a TCP/IP connection. The subordinate creates model input files using the parameters given by the master, runs the model, extracts the results from the model output files, and sends the simulation results back to the master. As a result, much of the computational load is offloaded to the subordinate computers and only the parameter estimation proper is left to the master. A schematic diagram showing how BeoPEST is run across the internet is shown in Figure 5.

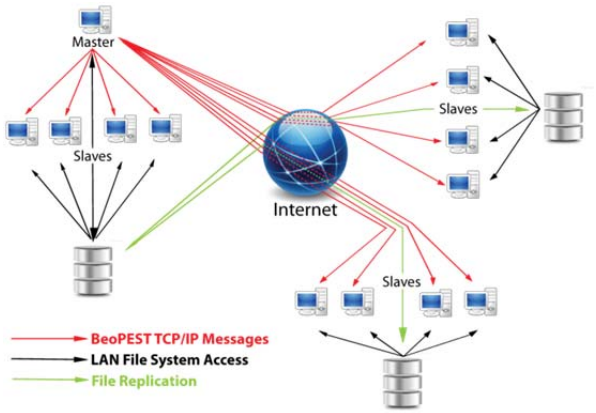

Figure 5: Schematic showing how BeoPEST is run across the internet (after Schreuder, 2009)

3.3 Avoiding local minimum

The minimization of the objective function based on the least-squares-error approach may not give a global optimum but may instead give a local optimum that may not be a "good solution" in the sense that the optimal parameters may not be what are expected or found to be acceptable by the modeller. In fact there may be several local optima that provide non-unique solutions to the model calibration problem. To rule out the possibility of local minima a grid search was performed across the range of possible values for the most important parameters.

4. MODELS OF DISCHARGE TEST

After some trials, well SKG9D was represented using one single porosity model and nine dual porosity (MINC) models. The different models that were investigated are summarised in Table 2.

In Model 1, a single porosity model was investigated with the following parameters optimised by PEST: permeability (k), porosity (θ), and initial pressure and gas saturation.

The MINC Models 2, 3, and 4, have a volume fraction of $1x10^{-3}$ assigned to the fracture and the remainder of the volume was assigned to 4 matrix blocks.

The MINC Models 5, 6, and 7, have a volume fraction of $1x10^{-3}$ assigned to the fracture and the remainder of the volume was assigned to a single matrix block.

The MINC Models 8, 9, and 10, have a volume fraction of $1x10^{-2}$ assigned to the fracture and the remainder of the volume was assigned to a single matrix block.

- In Models 2, 5, and 8, the matrix and fracture permeability (k_m, k_f), matrix porosity (θ_m), and initial pressure and gas saturation were estimated by PEST. The fracture porosity was set to be high (θ_f = 99%).
- In Models 3, 6, and 9, the matrix and fracture permeability (k_m, k_f), matrix porosity (θ_m), and initial pressure and gas saturation were estimated by PEST. The fracture was treated as a fracture zone and fracture porosity was fixed with θ_f = 10%.
- In Models 4, 7, and 10, the same parameters as in Models 2, 5, and 8 were given for PEST to estimate but the fracture porosity (θ_f) was allowed to vary and was also estimated by PEST. Moreover, Models 4, 7, and 10 were started with initial estimates of fracture porosity of 10%, 20%, 30%, 40%, 50%, 60%, 70%, 80%, and 99% to allow local minima to be identified.

5. PARAMETER ESTIMATION RESULTS

Single and dual porosity models were tested to determine which gave the best fit to the data. The model fit, measured by the value of the objective function, was compared to deduce which version of the model fits the data best.

Neither the single nor the dual porosity models were able to reasonably fit all the pressure drawdown data, especially the dip in wellbore pressure between day 55 and 70, as shown in Figure 6.

On the other hand, the single porosity model and the dual porosity MINC models all reasonably well fitted the flowing enthalpy data, as shown in Figure 7. The production rate decreased between days 85 to 95 while, as expected, the wellbore flowing pressure increased in the same period. Both the single porosity and dual porosity models were able to match the pressure and enthalpy data within this period.

The dual porosity model was able to reduce the objective function to a lower value than that obtained with the single porosity model. The objective function ranged from 461 to 595 for the dual porosity models compared to 1270 for the single porosity model. A comparison of the values of the objective function attained with each model is shown in Tables 3, 4 and 5. The lower objective function obtained with the dual porosity model corresponds to an improved fit to the observations for the dual porosity model as compared to the single porosity model. The results for the single porosity model and the best dual porosity model are shown in Figures 6 and 7. To simplify the figure, the results from the other MINC models, which are all very similar, were not included.

Table 2: Models of the Fushime discharge test

Model # type	Fracture volume fraction	MINC blocks	Parameters estimated
1 Single porosity	N/A	N/A	• permeability (k) • porosity (θ) • initial pressure • gas saturation
2 Dual porosity	$1x10^{-3}$	5	• matrix and fracture permeability (k_m, k_f) • matrix porosity (θ_m)[1] • initial pressure and gas saturation
3 Dual porosity	$1x10^{-3}$	5	• same as Model 2[2]
4 Dual porosity	$1x10^{-3}$	5	• same as Model 2 • fracture and matrix porosity (θ_f, θ_m) are parameters to be estimated by PEST
5 Dual porosity	$1x10^{-3}$	2	• matrix and fracture permeability (k_m, k_f) • matrix porosity (θ_m)[1] • initial pressure and gas saturation
6 Dual porosity	$1x10^{-3}$	2	• same as Model 5[2]
7 Dual porosity	$1x10^{-3}$	2	• same as Model 5 • fracture and matrix porosity (θ_f, θ_m) are parameters to be estimated by PEST
8 Dual porosity	$1x10^{-2}$	2	• matrix and fracture permeability (k_m, k_f) • matrix porosity (θ_m)[1] • initial pressure and gas saturation
9 Dual porosity	$1x10^{-2}$	2	• same as Model 8[2]
10 Dual porosity	$1x10^{-2}$	2	• same as Model 8 • fracture and matrix porosity (θ_f, θ_m) are parameters to be estimated by PEST

Notes:

(1) The fracture is treated as a highly porous single fracture with a fixed porosity θ_f = 99%.

(2) The fracture is treated as a fracture zone with a fixed porosity θ_f = 10%.

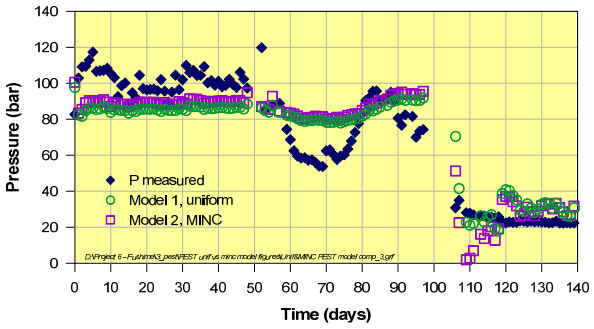

Figure 6: Feedzone pressure results: single porosity model and the best dual porosity model

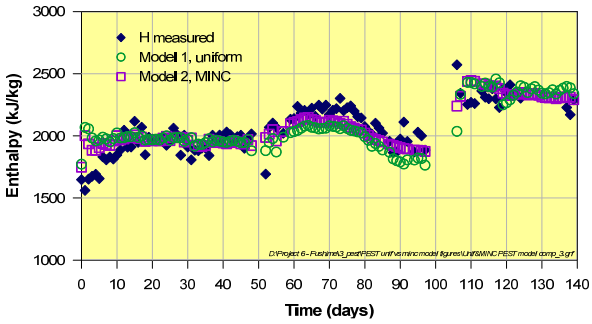

Figure 7: Flowing enthalpy results: single porosity model and the best dual porosity model

In Model 2, which has a fixed high porosity value assigned to the fracture (θ_f =99%), the fracture permeability decreased from 5mD to 2.78mD, matrix permeability decreased from 1mD to 0.41mD, matrix porosity decreased from 3.97% to 2%, initial pressure decreased from 115 bars to 103.4 bars, and initial gas saturation decreased from 25% to 22.4%. The composite observations (flowing enthalpy and wellbore pressure) are most sensitive to matrix porosity, followed by matrix and fracture permeability.

In Model 3, which has a fixed low porosity value assigned to the fracture (θ_f = 10%), the fracture permeability decreased from 5mD to 2.73mD, matrix permeability decreased from 1mD to 0.45mD, matrix porosity decreased from 3.97% to 2.95%, initial pressure decreased from 115 bars to 103.7 bars, and initial gas saturation decreased from 25% to 24.3%. The composite observations were sensitive to gas saturation, matrix porosity and matrix permeability at the early stages of optimisation.

In Model 4, which has the fracture porosity included as one of the parameters for inversion, the fracture permeability decreased from 5mD to 2.79mD, matrix permeability decreased from 1mD to 0.46mD, matrix porosity decreased from 3.97% to 2.79%, initial pressure decreased from 115 bars to 103.4 bars, and initial gas saturation decreased from 25% to 22.2%. Interestingly, the fracture porosity was pushed to 99% which was the highest value amongst the MINC models for which fracture porosity was estimated by PEST. The composite observations are most sensitive to matrix porosity and then to matrix permeability and matrix porosity.

In Model 5, which has θ_f = 99%, the fracture permeability decreased from 5mD to 3.1mD, matrix permeability decreased from 1mD to 0.13mD, matrix porosity decreased from 3.97% to 2.8%, initial pressure decreased from 115 bars to 97.5 bars, and initial gas saturation increased from 25% to 27.2%. The composite observations are sensitive to matrix porosity, matrix permeability, and initial pressure during the early stages of optimisation.

In Model 6, which has θ_f = 10%, the fracture permeability decreased from 5mD to 2.81mD, matrix permeability decreased from 1mD to 0.25mD, matrix porosity decreased from 3.97% to 2.68%, initial pressure decreased from 115 bars to 102.8 bars, and initial gas saturation decreased from 25% to 24.2%. The composite observations are sensitive to matrix porosity, matrix permeability, and gas saturation during the early stages of optimisation.

In Model 7, which also has the fracture porosity included as one of the parameters for inversion, the fracture permeability decreased from 5mD to 2.81mD, matrix permeability decreased from 1mD to 0.2mD, matrix porosity decreased from 3.97% to 2.68%, initial pressure decreased from 115 bars to 102.8 bars, and initial gas saturation increased from 25% to 25.4%. The fracture porosity was estimated to be 99%. The composite observations are most sensitive to fracture porosity and then to matrix permeability.

In Model 8, which has θ_f = 99%, the fracture permeability decreased from 5mD to 3.09mD, matrix permeability decreased from 1mD to 0.38mD, matrix porosity decreased from 3.97% to 1.8%, initial pressure decreased from 115 bars to 96 bars, and initial gas saturation increased from 25% to 27%. The composite observations are most sensitive to gas saturation and then to matrix porosity.

In Model 9, which has θ_f = 10%, the fracture permeability decreased from 5mD to 3.28mD, matrix permeability decreased from 1mD to 0.89mD, the matrix porosity decreased from 3.97% to 3.73%, initial pressure decreased from 115 bars to 95 bars, and initial gas saturation increased from 25% to 29.1%. The composite observations are sensitive only to fracture permeability.

Lastly in Model 10, which also has the fracture porosity included as one of the parameters for inversion, the fracture permeability decreased from 5mD to 3.30mD, matrix permeability decreased from 1mD to 0.18mD, matrix porosity decreased from 3.97% to 1.23%, initial pressure decreased from 115 bars to 94.5 bars, and initial gas saturation decreased from 25% to 23.9%. The fracture porosity was estimated to be 46.1%. The composite observations are most sensitive to matrix porosity and then to fracture porosity.

Among all the models, Model 4 gave the lowest value of the objective function (461). Model 4 is a 5-MINC model with which has the fracture porosity included as one of the parameters for inversion. Model 2 gave the next lowest value of the objective function (461.3). Model 2 is a 5-MINC model with a fixed high porosity value assigned to the fracture (θ_f =99%). Essentially, PEST drives Model 4 to be very similar to Model 2 but there is a problem with the occurrence of local minima as shown in Figure 8 where the final value of the objective function is plotted against the value of fracture porosity. The results from the single and all the dual porosity models are summarised in Tables 3, 4, and 5.

Table 3. Results of Parameter optimisation using PEST, fracture volume fraction $1x10^{-3}$, 5 MINC blocks

Model, type/ parameters	1 Single porosity	2 Dual porosity	3 Dual porosity	4 Dual porosity
Obj. f(x)	1270.4	461.3	494.5	**461.0**
k_f (mD)	2.99	2.78	2.73	2.79
k_m (mD)		0.41	0.45	0.45
θ_f (%)	8.99	***99.0***	***10.0***	***99.0***
θ_m (%)		2.0	2.95	2.0
P (bars)	98.9	103.4	103.7	103.4
Sg	0.26	0.224	0.243	0.222
Model rank	10	***2***	7	***1***

Table 4. Results of Parameter optimisation using PEST, fracture volume fraction $1x10^{-3}$, 2 MINC blocks

Model, type/ parameters	1 Single porosity	5 Dual porosity	6 Dual porosity	7 Dual porosity
Obj. f(x)	1270.4	484.5	482.4	462.9
k_f (mD)	2.99	3.10	2.81	2.81
k_m (mD)		0.13	0.25	0.20
θ_f (%)	8.99	***99.0***	***10.0***	***99.0***
θ_m (%)		2.82	2.68	2.68
P (bars)	98.9	97.5	102.8	102.8
Sg	0.26	0.272	0.242	0.254
Model rank	10	6	4	***3***

Table 5. Results of Parameter optimisation using PEST, fracture volume fraction $1x10^{-2}$, 2 MINC blocks

Model, type/ parameters	1 Single porosity	8 Dual porosity	9 Dual porosity	10 Dual porosity
Obj. f(x)	1270.4	514.3	595.3	482.9
k_f (mD)	2.99	3.09	3.28	3.30
k_m (mD)		0.38	0.89	0.18
θ_f (%)	8.99	***99.0***	***10.0***	***46.1***
θ_m (%)		1.8	3.73	1.23
P (bars)	98.9	96.0	95.0	94.5
Sg	0.26	0.270	0.291	0.239
Model rank	10	8	9	5

The lowest value for the objective function obtained from Models 2 (461.3), 4 (461), and 7 (462.9) were found to be very similar. All these models gave rise to a good fit between model output and field data and the estimated parameter values by these models are very similar. The parameters do not show a high degree of variability and do not take on extreme values. To investigate the best set of parameters further, a grid search was performed on Model 2 by varying fracture porosity but fixing matrix porosity, fracture and matrix permeability, and initial pressure and gas saturation conditions. The grid search went through a range of values of fracture porosity ranging from 10% to 99% for different values of matrix porosity ranging from 0.5% to 2.5%.

After doing a grid search, the highest value of the objective function obtained was 507.7 when the fracture porosity was 99%. As the matrix porosity decreased, the objective function was lowered until a minimum of 463 was obtained when fracture porosity was 99%. The result of the grid search is slightly different from the result of the PEST optimisation because the matrix porosity was not allowed to vary. The result of the grid search shows that the earlier PEST results gave the best parameter values for Model 2. However it also shows why, with different initial values for the fracture porosity PEST found a local rather than the global minimum.

The parameter estimation process using PEST tried to identify a region of the multidimensional parameter space where good models are likely to be found but it was found that this desirable region is adjacent to a region of parameter space where the forward model will not run until the desired end time. To investigate the parameter space near the problem zone more fully, a grid search was performed through a range of low matrix porosity values, namely: 2, 2.1, 2.2, 2.3, 2.4, and 2.5%. The plot of the objective function for different values of the fracture porosity is shown in Figure 8.

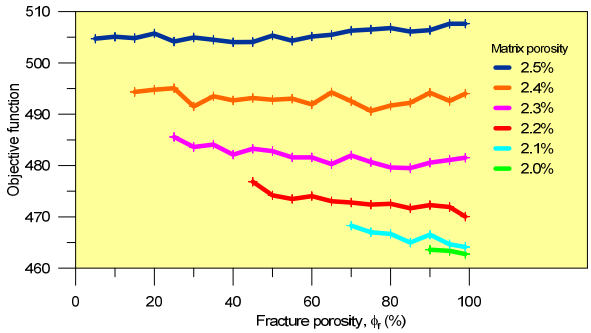

Figure 8: Result of a grid search showing the values of the objective function obtained by varying the fracture porosity and matrix porosity

The plots of pressure and flowing enthalpy results after the grid search at various fracture porosity values (5% to 99%) and matrix porosity values (2% to 2.5%) are shown in Figures 9 and 10. The value of 2% was the lowest matrix porosity for which some of the forward runs during grid search finished. There is no noticeable improvement in model fit as seen in Figures 9 and 10.

After trying several models, the ~30-bar dip in pressure between day 55 and 70 due to ~1.5 kg/s increase in mass extraction was not matched. The production wells in Fushime have multiple feed zones (Okada and Yamada, 2002) and the big dip in pressure may have been due to a change in feedzone contribution, or the cut-in of another feedzone when the pressure dropped, or a combination of both. It may be worth investigating whether or not a multi-feed model of well SKG9D can better fit the data.

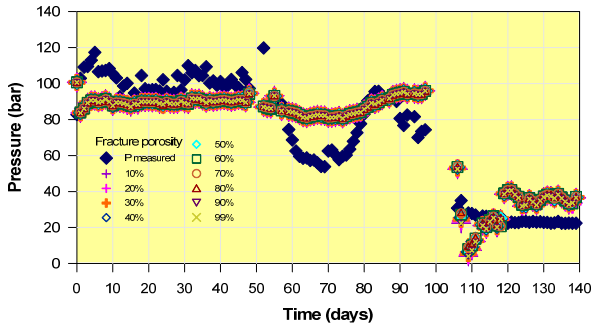

Figure 9: Feedzone pressure result using the best grid search parameters.

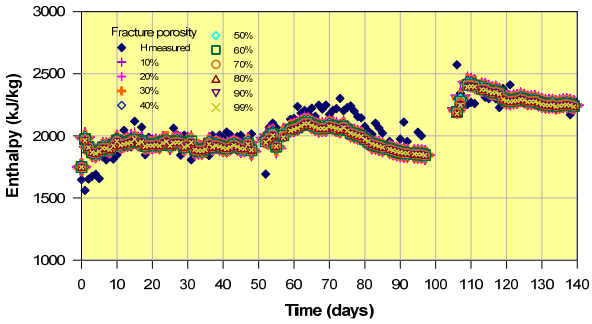

Figure 10: Flowing enthalpy results using the best grid search parameters

6. CONCLUSIONS AND RECOMMENDATIONS

All the dual porosity models used to simulate the discharge test of well SKG9D were able to reduce the objective function to a lower value than that for the single porosity model. The results of PEST optimisation showed that discharge test is marginally better modelled using a single high porosity fracture. Dual porosity Model 4, which gave the lowest value of the objective function (461), was estimated by PEST to have a single high porosity fracture (θ_f =99%). Similarly, Models 2 and 7 which gave the second and third lowest value of the objective function at 461.3 and 462.9 respectively also have a fixed high porosity value assigned to the fracture (θ_f =99%).

However, the value of the objective function for the other dual porosity models was not much higher and the results produced are very similar. For example, the result of PEST optimisation suggested that the discharge test can also be modelled by treating the fracture as a fracture zone rather than a single high porosity fracture as Model 6 with fracture porosity included as one of the parameters for inversion gave the fourth lowest value of the objective function (482.4) and a fracture porosity of 10%.

Both the single and dual porosity models have difficulty in simulating the relatively large drop in wellbore pressure between day 55 and 70. The ~30-bar drop in pressure associated with a ~1.5 kg/s increase in mass is a feature of the measured data that the model cannot match. However, both single and dual porosity models reasonably fitted the flowing enthalpy data over the entire duration of the discharge test. It may be necessary to use a more complex multi-feed model to obtain a better match to the data.

ACKNOWLEDGEMENTS

The first author would like to thank the Energy Development Corporation for supporting this PhD study.

REFERENCES

Austria, J.J.C. and O'Sullivan, M.J., 2012. Dual porosity models of near-well behaviour of a discharging well, *New Zealand Geothermal Worskhop 2012*, Auckland, New Zealand.

Barenblatt, G.I., Zheltov, I.P. and Kochina, I.N., 1960. Basic concepts in the theory of seepage of homogeneous liquids in fissured rocks. *Journal of Applied Mathematical Mechanics*, 24(5): 1286-1303.

Croucher, A.E., 2011. PyTOUGH: a Python scripting library for automating TOUGH2 simulations, *Proceedings 33rd New Zealand Geothermal Workshop*.

Doherty, J., 2013. PEST: Model-Independent Parameter Estimation. Watermark Numerical Computing, Brisbane.

Finsterle, S., 2003. iTOUGH2: From parameter estimation to model structure identification, *Proceedings, TOUGH2 Symposium 2003*, Lawrence Berkeley National Laboratory, Berkeley, California.

Narasimhan, T.N., 1982. Multidimensional numerical simulation of fluid flow in fractured porous media. *Water Resources Research*, 18(4): 1235-1247.

Okada, H. and Yamada, Y., 2002. Fracture distribution in and around intrusive rocks in the Fushime Geothermal Field, Japan: Evidence from FMI Logging, *Society of Petrophysicists and Well-Log Analysts Annual Logging Symposium*, 2002.

Okada, H., Yasuda, Y., Yagi, M. and Kai, K., 2000. Geology and fluid chemistry of the Fushime geothermal field, Kyushu, Japan. *Geothermics*, 29(2): 279-311.

Pritchett, J.W., 2005. Dry-steam wellhead discharges from liquid-dominated geothermal reservoirs: A result of coupled nonequilibrium multiphase fluid and heat flow through fractured rock. *Geophysical monograph*, 162: 175-181.

Pruess, K., 2010. GMINC - A Mesh Generator for Flow Simulations in Fractured Reservoirs. Lawrence Berkeley National Laboratory, LBNL Paper LBL-15227.

Pruess, K. and Narasimhan, T.N., 1982. On fluid reserves and the production of superheated steam from fractured, vapor-dominated geothermal reservoirs. *Journal of Geophysical Research*, 87(B11): 9329-9339.

Pruess, K., Oldenburg, C. and Moridis, G., 1999. TOUGH2 User's Guide, version 2.0. Lawrence Berkeley National Laboratory.

Schreüder, W., 2009. Running BeoPEST. Principia Mathematica. Document can be found via the following website address: http://www. prinmath. com.

Warren, J. and Root, P.J., 1963. The behavior of naturally fractured reservoirs. *Old SPE Journal*, 3(3): 245-255.

Yeh, A., Croucher, A.E. and O'Sullivan, M.J., 2012. Recent Developments in the AUTOUGH2 Simulator, *Proceedings TOUGH2 Symposium 2012*, Berkeley, California.